J. Phys IV France **12** (2002)
© EDP Sciences, Les Ulis
DOI. 10.1051/jp4:20020245

X-ray reflectivity investigations of two-dimensional assemblies of C-cadherins: First steps in structural and functional studies

L. Martel, C. Johnson[1], S. Boutet[2], R. Al-Kurdi[3], O. Konovalov[4], I. Robinson[2], D. Leckband[1] and J.-F. Legrand

UMR 5819 du CEA-CNRS, Université J. Fourier, Département de Recherche Fondamentale sur la Matière Condensée, CEA/Grenoble, 17 avenue des Martyrs, 38054 Grenoble cedex 9, France
[1] *Center for Biophysics and Computational Biology, Departments of Biochemistry, Chemistry and Physics, 600 S. Mathews Ave., Urbana, IL 61801, U.S.A.*
[2] *Department of Physics, University of Illinois, AT Urbana-Champaign, 1110 West Green Street, Urbana, IL 61801-3080, U.S.A.*
[3] *Institut de Biologie Structurale, Laboratoire d'Ingénierie des Macromolécules, 41 avenue des Martyrs, 38027 Grenoble cedex, France*
[4] *ESRF, 6 rue Jules Horowitz, BP. 220, 38043 Grenoble cedex, France*

Abstract: Cadherins are transmembrane proteins involved in cell adhesion. They play a major role in recognition and adhesion between adjacent cells via calcium dependent interactions. Our studies aim at determining the laws of assembly of cadherins and locating the adhesive interactions along the proteins, starting from low-resolution structures obtained by X-rays grazing incidence reflectivity. We have realized monolayers of the extracellular fragment of C-cadherin of the frog *Xenopus*, anchored to nickel chelating lipids at the water surface. From X-ray reflectivity measurements carried out at ESRF, we have elaborated profiles of the electron density of the proteins along their axis with 0 9 nm resolution We have studied their adhesive behaviour with high and low calcium concentrations and we show an ordering of the protein above 1 mM of calcium We present an attempt to locate the binding of a short fragment of cadherin on the full-length protein The complementarities of our results with those of biochemical studies should enable us to comprehend further cellular adhesion mechanisms

Résumé: Les cadhérines sont des protéines transmembranaires impliquées dans l'adhésion cellulaire. Elles jouent un rôle majeur dans la reconnaissance et l'adhésion entre cellules contiguës via des interactions dépendantes du calcium. Nos études visent à déterminer les lois d'assemblage des cadhérines et à localiser les interactions adhésives le long des protéines, à partir de structures à basse résolution obtenues par réflectivité des rayons X en incidence rasante Nous avons réalisé des monocouches de fragments extracellulaires de C-cadhérine de la grenouille *Xenopus*, ancrés à des lipides chélateurs d'un ion nickel déposés à la surface de l'eau A partir de mesures de réflectivité des rayons X effectuées à l'ESRF, nous avons déterminé des profils de densité électronique des protéines le long de leur axe avec une résolution de 0.9 nm. Nous avons étudié leur comportement adhésif à faible et haute concentration en calcium, et nous montrons que la couche de protéine s'ordonne au-dessus de 1 mM de calcium Nous présentons également une tentative de localisation de l'interaction

d'un fragment de C-cadhérine plus court sur la protéine entière La complémentarité de nos résultats avec ceux d'études biochimiques devrait nous permettre d'avancer dans la compréhension des mécanismes de l'adhésion cellulaire

1. Introduction

Cadherins are transmembrane glycoproteins involved in adhesive junctions between cells [1]. They are extremely important proteins as they participate in tissue formation and maintenance by means of precise molecular recognition [2,3,4]. There exist several families of cadherins belonging to different types of cells, which permit the sorting of cells especially during embryogenesis. Dysfunctions of their activity can lead to severe damage to the tissue integrity and they are involved in many cancer development. Their adhesive function is related to their molecular structure and an atomic description of cadherins would be of great interest for medical purposes as well as from a fundamental point of view [5]. The different types of cadherins share common features: a cytoplasmic part involved in cellular communication and an extra-cellular part, consisting in five homologous domains, which are assumed to control the adhesive interactions. An important characteristic of the interactions between cadherins is their dependence upon calcium concentration. The atomic structure of one or two domains [6, 7, 8, 9] brought to light interesting pieces of information but to date, the mechanism of the adhesive interaction between cadherins remains unclear. Several models have been proposed to describe these interactions based on the three dimensional structures of fragments of cadherins and on biochemical analyses [10, 11, 12, 13, 14, 15], but they generally suffer from a lack of direct information on the structure of the complete adhesive complex.

The aim of this study is to obtain structural information using a model system based on a monolayer of extracellular fragments of cadherins anchored to a lipid layer at the air-water interface. It is constructed with cadherin ectodomains expressed with a polyhistidin tag at the C-terminus and consequently able to bind nickel chelating lipids. Such a monolayer is able to bind other fragments injected in the subphase for locating the interacting parts of the protein along its long axis. This model system thus mimics a cell membrane. It also allows the control of the surface pressure and concentration of ligand lipids in the layer. We report on results obtained with recombinant fragments of C-cadherin from *Xenopus*. Ellipsometry measurements were used to monitor the formation of monolayers and protein complexes. X-ray reflectivity measurements were used to analyse the changes in the electron density profile perpendicular to the interface. Using a synchrotron X-ray source, a resolution up to 0.9 nm can be obtained in the structure of the molecular layers at the air-water interface [16, 17]. We show how the structure of the monolayers of cadherins can provide functional information on the formation of calcium dependent complexes.

2. Experimental

2.1. Chemicals

The recombinant fragment of C-cadherin (CEC1-5) of the African frog *Xenopus* was overexpressed and purified as described elsewhere [11, 18]. It consists in the complete extracellular part of the protein, that is the five ectodomains plus a hexahistidin tag at the C-terminus (total M_W : 70 kDa). The domains are numerated from 1 at the N-terminus to 5 at the C-terminus. A second fragment of C-cadherin was used: a chimera protein of the first three domains (CEC1-3) linked to an IgG Fc domain in C-terminus (Fc-CEC1-3). Fc fragments form parallel dimers via disulfide bonds and these C-cadherin fragments are thus in the form of dimers in solution [11].

The C-cadherins were purified and kept in a buffer made of 50mM Tris-HCL, 100mM NaCl in ultra-pure water with a pH 7. 5. Different calcium concentrations were used to study the interactions between cadherins: 0.1 mM, 1mM and 2.5mM of $CaCl_2$. The working concentration of protein CEC1-5 was about 0.5 μM. Fc-CEC1-3 was added in excess at a ratio of 1.3 to CEC1-5 concentration. Nickel chelating lipids Ni-NTA-DLGE (6-[9-[2,3-bis(dodecyloxy)propyl]-3,6,9-trioxanonyl-1-oxycarboxylamino]-2-[di(carboxylmethyl)-amino]-hexanoic acid) were purchased from Northern Lipids (Vancouver, Canada). They were dissolved in $CHCl_3$ to form a spreading solution of 1. 36 mg/ml. $NiCl_2$ was added in some experiments to saturate lipid head groups. All measurements were made at room temperature.

2.2. *Preparation of a protein monolayer*

The experiments were performed in Teflon troughs of 3ml for ellipsometry measurement, and of 15ml for X-ray reflectivity experiments. The troughs were either cleaned using boiling HCl: H_2O_2: H_2O (1:1:1 v: v: v) for about 20 minutes then rinsed with pure water; or cleaned with chloroform, ethanol, and pure water.

Ligand lipid solutions were spread on the buffer surface and the surface pressure was controlled by a Whilhelmy balance (NIMA, England). They were deposited at a surface pressure just before collapse, typically about 30mN/m for Ni-NTA-DLGE. Proteins were injected in the subphase via capillaries connected to a small hole in the trough and a monolayer of proteins formed at the surface within a few hours. At the beginning of incubation the subphase was circulated by means of a peristaltic pump at a mean flow rate of 0. 5ml/min. This was found to enhance the kinetics of adsorption of the protein and the chance obtaining a homogeneous protein layer. The reflectivity signal was measured after a few hours, allowing for a maximum adsorption of proteins to the lipids.

2.3. *Reflectivity set-up*

The X-ray reflectivity measurements were performed at beamline ID10B, ESRF, France. The set-up of the monochromator and of the reflectivity instrument are described elsewhere [19]. The wavelength used was 1.537 Å. The horizontal and vertical apertures were respectively 1 mm and 0.1mm before the sample. The surface of the trough was 80*60 mm^2 respectively along the beam path and perpendicular to it. With this choice, the footprint of the X-ray beam on the sample surface was smaller than the length of the trough at the critical angle of total reflection with the chosen slits (the footprint of the beam was 37.6 mm at the critical angle of water at this energy, α_c= 0.1522°). Secondly, in order to avoid beam damage to the protein [20], the width of the trough was large enough for a translation perpendicularly to the beam path during the measurement. The trough was placed in a cell filled with helium to reduce the small angle scattering of X-rays on air and to reduce oxidation of the sample due to ozone formed by X-ray in the air. The specular reflection was recorded in the range from 0 to 2.5 degrees (0 3567 $Å^{-1}$) via a position sensitive detector (PSD) oriented parallel to the plane of incidence that allows afterwards subtracting parasitic background at each point. A set of aluminium foils of different thickness was used to absorb photons at small incidence angle and to protect the detector from damage or saturation. A complete reflectivity curve measurement lasted about one hour. The trough was translated at large incidence angle when no aluminium absorption plate was used: the total exposure time per sample area was between 75 seconds and 140 seconds.

The level of water was controlled by two methods during a full reflectivity curve measurement A water level controller (Nanofilm GmBH, Germany) was used to compensate

for the evaporation and to regulate the water level within 10μm of accuracy. A more accurate positioning of the surface with respect to the beam was made by a scan of the whole cell height prior to and twice during each measurement. Two antivibration stages (MOD-2, Halcyonics) supported the trough to reduce capillary waves at the water surface.

2.4. Ellipsometry

Ellipsometry measurements at the water surface were made with a photoelastic modulation ellipsometer (Jobin-Yvon Ltd, UK). The working wavelength was 459.3 nm. Measurements of the ellipsometric angle Δ, at fixed incidence angle with respect to the vertical (53°5, i.e. 0.5° beyond the Brewster angle for water), was used to follow the kinetics of adsorption of the protein to the ligand-lipid monolayer.

3. Results

In order to analyse the structure of a protein along its axis perpendicular to the air-water interface by X-ray reflectivity, the protein should form a dense monolayer at the surface. The optimal initial protein concentration and incubation time were determined by ellipsometry.

We present here three significant reflectivity curves of C-cadherin CEC1-5 layers anchored to the lipids Ni-NTA-DLGE.

- Layer A was made of densely packed cadherins CEC15 in a 1 mM calcium buffer.
- Layer B contained the same protein with only 0 1 mM $CaCl_2$. It was studied to explore the effect of lack of calcium ions on the structure along the cadherin.
- Layer C was an attempt to form complexes of cadherin CEC15 with pairs of the fragment Fc-CEC1-3. The fragments were injected in the subphase after obtaining a layer of protein CEC1-5 with high calcium concentration (2.5mM).

3.1. Control of adsorption by ellipsometry

Figure 1 shows the kinetics of adsorption of C-cadherin to a monolayer of NI-NTA-DLGE lipids in a 0.1 mM $CaCl_2$ buffer. For other calcium concentrations the kinetics are very similar. The time needed to obtain a dense layer is about 5 hours. After deposition of the lipids up to a surface pressure of 30mN/m the angle Δ jumped to 37 degrees. This value is set to 0 on the graph. The proteins are then injected in the subphase and the timescale is set to zero. The angle Δ increases gradually during 4 hours to reach a plateau at 66 degrees and remains stable for hours. The oscillations at the beginning of the experiment correspond to inhomogeneity of the layer as seen by the beam. The beam diameter is 4mm while the trough diameter is 50 mm.

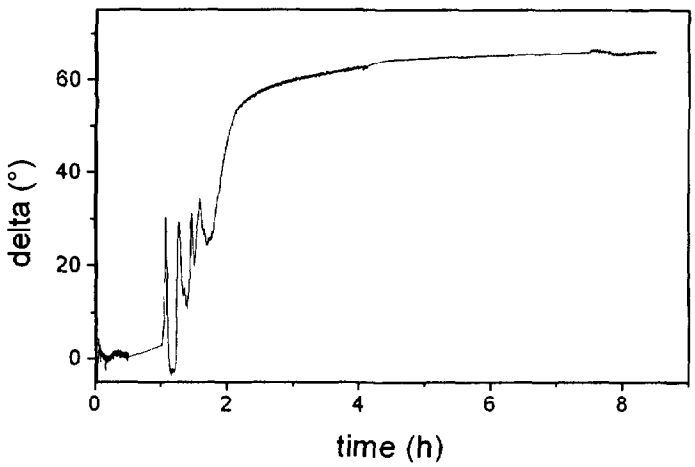

Figure 1 : Kinetics of adsorption of C-cadherin CEC1-5 to a monolayer of NI-NTA-DLGE lipids in a 0.1 mM $CaCl_2$ buffer Cinétique d'adsorption de la C-cadhérine CEC1-5 à une monocouche de lipides NI-NTA-DLGE dans un tampon à 0.1 mM $CaCl_2$

3.2. X-ray reflectivity

A reflectivity measurement on a pure NI-NTA-DLGE lipid monolayer was monitored prior to the injection of protein (Figure 2). The reflectivity signal is multiplied by q_z^4, that to compensate for an asymptotic approximation to Fresnel law at $q_z > q_c$, to enhance the oscillations (Kiessig fringes). Figure 3, Figure 4 and Figure 5 show the reflectivity curves corresponding to layer A, B and C respectively.

In Figure 2, the modulation showing a minimum around q=0.21 $Å^{-1}$ is due to the lipid monolayer and corresponds to a total thickness of 30 Å. To analyse the data we have used a classical electron density model of layers that describes the system. The parameters of the model have been adjusted to give the best agreement between the experimental and calculated reflectivity curves with the fitting program *Parratt32* [21]. This fitting procedure gives a good agreement between experimental and calculated data for the lipid monolayer, as shown by the Figure 2. The lipids are modelled with a three-layer model (see below). For comparison, the electron density of water is taken to be 0.334e.$Å^{-3}$.

i) Aliphatic chain: thickness t_{chain}=14.5Å, electron density ρ_{chain}=0.26e.$Å^{-3}$ and roughness σ_{chain}=4Å;

ii) Head group: t_{head}15.8 Å, ρ_{head}=0.54 e.$Å^{-3}$ and σ_{head}=5 Å;

iii) End of spacer with nickel: t_{spacer}7.3 Å, ρ_{spacer}=0.4e.$Å^{-3}$ and σ_{spacer}=3 Å.

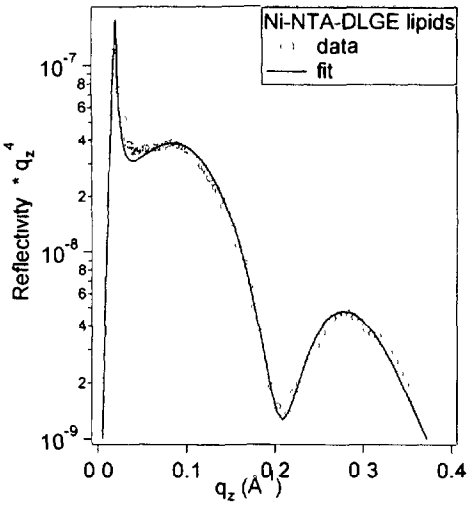

Figure 2 : Reflectivity curve on pure Ni-NTA-DLGE lipids. Courbe de réflectivité sur des lipides seuls Ni-NTA-DLGE.

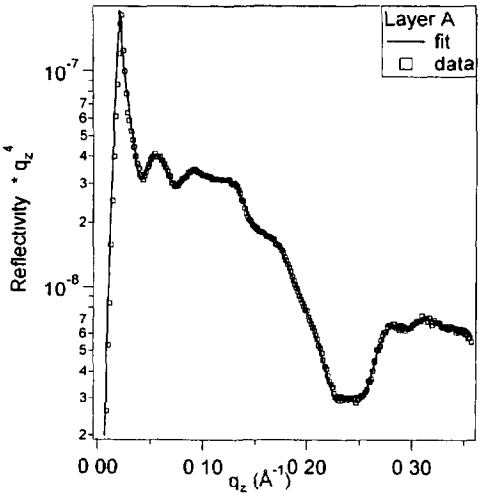

Figure 3 . Layer A : a reference curve with CEC1-5, 1 mM $CaCl_2$ Couche A : courbe de référence avec CEC1-5, 1 mM $CaCl_2$

In the next figures, 3, 4 and 5, the main modulation showing a minimum around q=0.23 Å^{-1} is also due to the lipid monolayer and corresponds to a thickness of about 27 Å. The lipid thickness is here smaller than the thickness of the bare lipid monolayer. This change is interpreted as follows: the protein histidine-tag interacts with the nickel group and this part of the lipid enters in the protein contribution. The secondary oscillations of q-period 0.037 Å^{-1} are associated with the protein and correspond to a thickness of about 170 Å. The position of the minimum in q-space for the lipids does not change from one curve to another, but the

constructive and destructive interferences with the protein contribution shape the bottom of the minimum. The amplitude of the oscillations due to the protein layer varies for the different experimental conditions A, B and C, which already suggests a difference of protein surface density in these layers.

It turned out to be very difficult to describe the protein layer with a simple layer model. Instead, we have used a fitting program written by R. Ober [22] where the electron density profile represented by a series of equally thick small slabs. The slab thickness is chosen of the order of the experimental resolution, i.e. 10 Å. Only the electron density of the slabs is fitted while the width and the roughness of each slab are kept constant. With this limited increase of the number of fitting parameters, we obtained a smooth electron density profile that gives a good agreement between experimental and calculated reflectivity curves for all analysed samples. In all electron density profiles shown here, the distance 0 corresponds to the air-monolayer interface and positive distances increase in the layer.

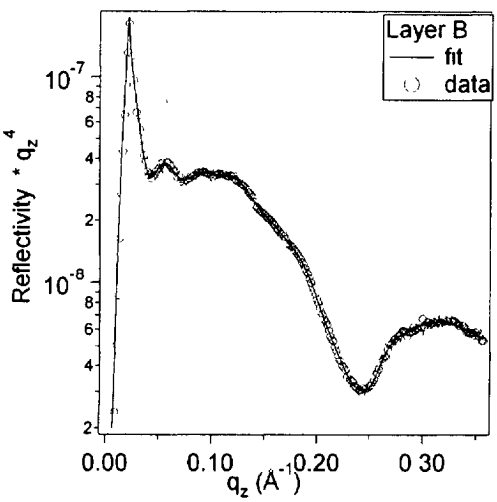

Figure 4 Layer B : following the effect of low calcium concentration, CEC1-5, 0.1 mM $CaCl_2$. Couche B : suivi des effets d'une faible concentration en calcium, CEC1-5, 0.1 mM $CaCl_2$

Figure 6 shows the electron density profile for layer A (CEC1-5, 1 mM $CaCl_2$). The electron density shows a peak of high density (0.486 e.$Å^{-3}$) with a width of 20 Å corresponding mainly to the lipid head group. A plateau of mean density 0.373 e.$Å^{-3}$ is attributed to the protein monolayer. The proteins and the lipids interpenetrate making the real separation of their respective contribution impossible. The electron density profile decreases slowly down to the water electron density (0.334 e.$Å^{-3}$) from a depth of 170 Å to 220 Å. The total thickness of the layer is therefore about 180 Å. After subtracting the lipid thickness, the protein monolayer is about 150 Å thick. The small minimum at around 105 Å depth suggests that the protein monolayer is divided into two parts of 75Å. The first part is of higher mean density but decreases from 0.405 e.$Å^{-3}$ to 0.375 e.$Å^{-3}$. The density of the second part is rather flat, having a mean value of 0.38 e.$Å^{-3}$.

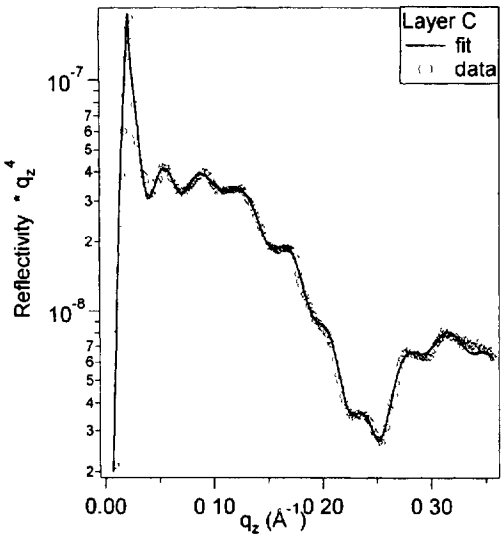

Figure 5 Layer C· evidence of possible binding of a fragment to the full cadherin . CEC1-5 and fragment Fc-CEC1-3, 2 5 mM $CaCl_2$ Couche C. analyse d'une possible interaction d'un fragment à la cadhérine entière · CEC1-5 et le fragment Fc-CEC1-3, à 2.5 mM $CaCl_2$.

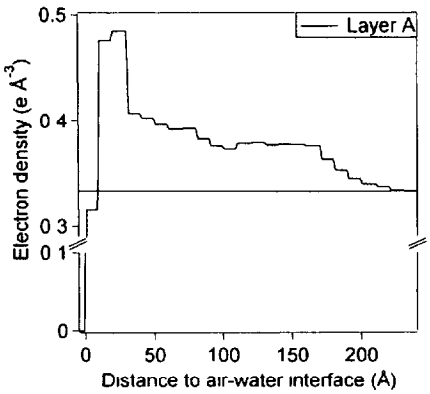

Figure 6: Model of electron density profile for layer A (CEC1-5, 1 mM $CaCl_2$). Modèle de profil de densité électronique pour la couche A (CEC1-5, 1 mM $CaCl_2$).

Figure 7 (a and b) presents the models of electron density profiles obtained for the curves B and C. The electron density profiles show the same feature for the three layers: the total thickness is about 180Å and the mean density is 0.372 e.$Å^{-3}$ for layer B and 0.371 e.$Å^{-3}$ for layer C. However, the minimum seen at a depth of 105 Å on the layer A and B profiles is not so clearly visible for layer C profile. The electron density of this layer is flatter, while the profile for layer B decreases smoothly to the electron density of water.

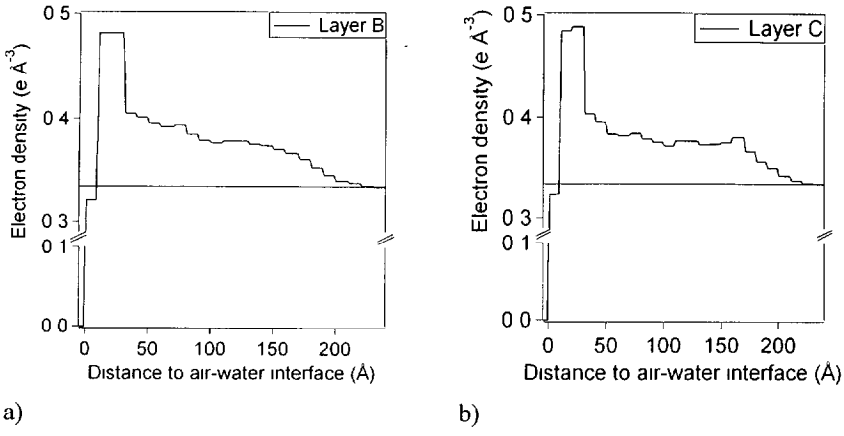

Figure 7 a) model of electron density profile for layer B (CEC1-5, 0 1 mM $CaCl_2$) b) model of electron density profile for layer C (CEC1-5 and fragments Fc-CEC1-3, 2 5 mM $CaCl_2$) a) modèle de profil de densité électronique pour la couche B (CEC1-5, 0 1 mM $CaCl_2$) b) modèle de profil de densite electronique pour la couche C (CEC1-5 and fragments Fc-CEC1-3, 2 5 mM $CaCl_2$)

4. Discussion

Figure 8 shows the protein fraction in the layer A, assuming a protein mean electron density of 0.448 e.Å^{-3} [23]. With this hypothesis, the average percentage of protein in the layer is 34%, which corresponds to a relative close packing of the protein (for a three dimensional crystal of protein, the percentage of protein varies from 25% to 70%, the rest being the buffer [23])

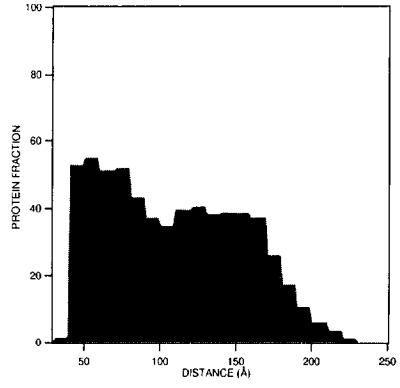

Figure 8 Fraction of protein in the total electron density for layer A (CEC1-5, 1 mM CaCl2) The fraction ϕ of protein in the layer is given by $\rho_{exp}=\phi\rho_p+\rho_w(1-\phi)$, where ρ_{exp} is the measured electron density, ρ_p the dry protein mean electron density (0 448 e Å^{-3}) and ρ_w the electron density of water (0 334 e Å^{-3}). The lipid contribution was subtracted at short distance (below 5 nm). Fraction de proteine de la densité électronique totale pour la couche A (CEC1-5, 1 mM CaCl2) La fraction ϕ de protéine dans la couche est donnée par $\rho_{exp}=\phi\rho_p+\rho_w(1-\phi)$, où ρ_{exp} est la densité électronique mesurée, ρ_p la densité électronique de la protéine sèche (0 448 e.Å^{-3}) et ρ_w la densité électronique de l'eau (0 334 e Å^{-3}) La contribution de lipides est soustraite à courte distance (inférieure a 5 nm)

The model of Figure 8 displays an average thickness of the cadherin layer of about 140Å. Taking a fully extended cadherin length of 220Å into account [24], this result clearly shows that the proteins are not perpendicular to the surface but have instead a mean tilt angle of 50

degrees with respect to the vertical direction. The layer is thus likely heterogeneous with patches of proteins of various orientations Some proteins could be bent back towards the lipids explaining the increase of the protein fraction close to the lipid layer and the roughness-like decrease between depth 170 Å and 220 Å. The fact that the thickness of the cadherin layer is approximately the same for the different calcium concentration (i.e. the existence of dimers or monomers) proves that, if there is a monolayer of trans-dimers, they are totally interpenetrated

4.1. Calcium dependence

There are three calcium binding sites between each pair of domains leading to a total of 12 calcium ions per protein. According to a recent study on E-cadherin [6], the affinity constants of calcium are different for each site and the formation of an adhesive junction under increasing [Ca^{2+}] concentration would develop in several steps, as sketched in Figure 9. At a low calcium concentration (below 0.05 mM), the protein is unfolded. Above this threshold, the cadherin is folded but is unable to associate with another cadherin (between 0.05 and 0.5 mM). The cadherins would associate in parallel dimers, also named *cis*-dimers, when all calcium sites are occupied apart from one at the N-terminus site (between 0.5 and 1 mM). This last calcium binding would permit the proteins to associate in an adhesive complex formed by two *cis*-dimers linked in antiparallel or *trans*-dimers.

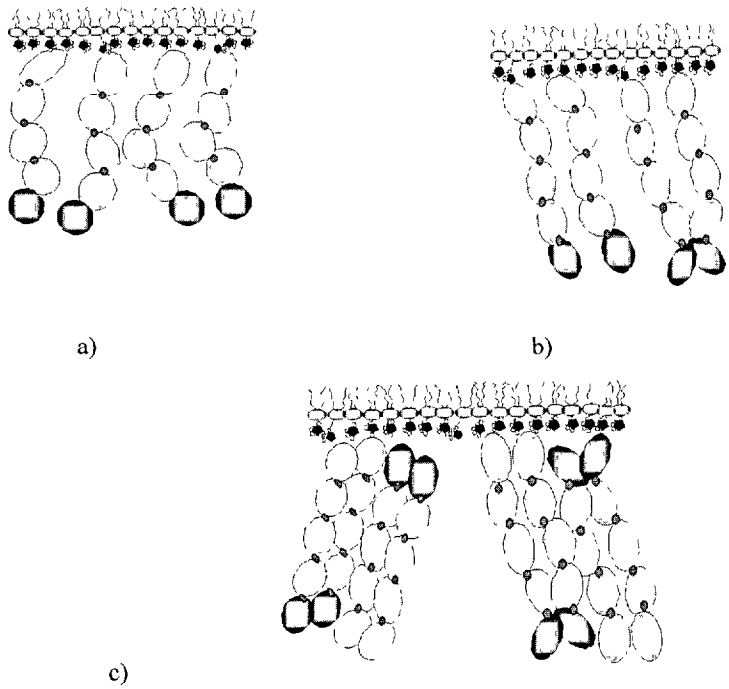

Figure 9 Schematic model of cadherin interaction at different calcium concentration a) At low calcium cadherins don't interact b) At medium calcium concentration cis-dimers may form c) High calcium concentration, trans-dimers should appear Schémas des modèles d'interaction entre cadhérines à différentes concentrations en calcium a) A faible concentration en calcium les cadhérines n'interagissent pas entre elles b) A une concentration en calcium intermédiaire, il peut se former des dimères latéraux ou *cis* c) A concentration en calcium elevée, des dimères antiparallèles ou *trans* devraient apparaître

Layer A consists of full CEC1-5 in a 1 mM CaCl2 buffer compared to 0.1mM for layer B. The only noticeable change in the electron density profiles we calculated appears in the deeper region. There is a shoulder in the electron density of layer A at a depth of 170 Å, which is not present in the low calcium profile (layer B). We explain this as a partial organisation of the layer due to the calcium. With a low calcium concentration, the cadherin layer is not homogeneous as far as the density along its axis is concerned. The cadherins are assumed to present a large variety of orientations with respect to the surface and also from one domain to another (shown schematically by Figure 9a). They are not rod-like, but present an internal flexibility. This explains the smooth electron density profile with a higher density at low depth and the slow decay of electron density profile towards the density of water. With a higher calcium concentration, the cadherins may interact associating in *cis*- or *trans*-dimers. This organisation inside the monolayer (Figure 9b and c) is leading to the much flatter electron density profile observed. It is possible that the shoulder around 150Å reflects a *cis* interaction between domains 1 of cadherins as shown schematically in Figure 9b [6].

4.2. *Fragment binding: cadherin interaction with fragments?*

If there were any binding of the fragments to the full cadherin, we would expect to see large change in the reflectivity curve of layer C and its corresponding electron density profile (Figure 5 and Figure 7b). The layer should be thicker even if the fragments CEC1-5 and CEC1-3 interpenetrate because of the presence of the Fc fragments of about 45 Å long. We would thus expect to see an oscillation of smaller period in the reflectivity curve or a more complex set of oscillations. The injection of fragments was performed at a calcium concentration of 2.5mM, which is necessary to induce cadherin interactions. However, the affinity constants between cadherins of different lengths are not the same [11]. It is thus possible that the full cadherins CEC1-5 preferably form *trans*-dimers and the fragments Fc-CEC1-3 are expulsed from the layer.

Nevertheless, the electron density profile is slightly different from the ones obtained for layer A and B. The profile is much flatter which leads us to conclude that in this layer, the proteins are well aligned, as sketched by Figure 9c. If the hypothesis of fragment binding is put aside, the main remaining difference between the layers is the incubation time: layer A was incubated for 5 hours whereas layer C was incubated for more than 24 hours. The cadherins of layer C had therefore a longer time to become rigid and organise themselves. Because of the presence of calcium in the buffer, the proteins are able to interact with each other and may form *cis* and/or *trans*-dimers. The flat electron density profile obtained is interpreted in terms of an ordering in the layer: because they interact, cadherins are not free to move anymore and the subsequent profile is constant. We do not see yet any precise features of domains: this would happen only if the proteins were in perfect registry. It could also be related to the existence of *trans*-dimers: the electron density modulation that the five domains would create disappears and we actually see a mean value of the electron density.

5. Conclusion

We presented here the relevance of using X-ray reflectivity for studying at the same time the low-resolution structure of proteins and the interactions of proteins with each other. A range of momentum transfer from 0 to 0.3Å^{-1} provides sufficient resolution for probing biological interactions at the scale of protein domains.

We have compared the structure of C-cadherins at high and low calcium concentrations. This showed the increase of structural ordering of cadherins with increasing incubation time and calcium concentration. The different electron density in the low calcium layer can be interpreted in terms of a relative disorder. We followed cadherin interactions with each other but the interaction of the cadherin CEC1-5 and the short fragment Fc-CEC1-3 could not

be seen. This was probably due to an overly dense layer of cadherins at the surface and a much higher affinity for cadherin fragments of the same length than for shorter species.

In order to locate the binding of a short fragment on the full-length cadherin two strategies are conceivable for a future experiment. A first strategy is to have completed the association between full-length and short fragments before the injection of the complex in the subphase. A large excess of short fragments with respect to the full-length cadherin would be necessary to favour the formation of heterodimers. In a second procedure, the aim is first to visualise the full-length cadherin layer structure and then to follow the interaction with the shorter fragment. In this case, it would be necessary to detach any possible *trans*-dimers by diluting the buffer and reaching a low calcium concentration, before injecting the short fragment and adding calcium. Such a set of experiments should allow us to locate the interaction of cadherin domains with respect to each other.

6. Acknowledgements

We would like to acknowledge B. Gumbiner (Memorial Sloan-Kettering Cancer Center, New York, USA) for generous gifts of cadherins. We thank S. Sivasankar (University of Illinois at Urbana-Champaign), D. Gulino and P Legrand (Institut de Biologie Structurale, Grenoble, France) for helpful discussions.

References

[1] M. Takeichi, Science **251**, 1451-1455 (1991)

[2] B. Gumbiner, J Cell Biol. **148**, 399-404 (2000)

[3] K. Vleminckx, R. Kemler, Bioassays **21**, 211-220 (1999)

[4] B Gumbiner, Cell **84**, 345-357 (1996)

[5] A. Ben-Ze'ev, Curr Opin Cell Biol **9**, 99-108 (1997)

[6] O. Pertz *et al.*, EMBO **18**, 1738-1741 (1999)

[7] B. Nagar *et al.*, Nature **380**, 360-364 (1996)

[8] L. Shapiro *et al.*, Nature **374**, 327-336 (1995)

[9] M. Overduin, *et al.*, Science **267**, 386-389 (1995)

[10] R. Iino, I. Kyoama, A. Kusumi, Biophys. J. **80**, 2667-2677 (2001)

[11] S. Chappuis-Flament, J Cell Biol **154**, 231-243 (2001)

[12] S. Sivasankar, B. Gumbiner, D. Leckband, Biophys J **80**, 1758-1768 (2001)

[13] P. Legrand *et al.*, J Biol Chem **276**, 3581-3588 (2001)

[14] A. Koch *et al.*, Biochem **36**, 7697-7705 (1997)

[15] A. Tomschy *et al.*, EMBO J **15**, 3507-3514 (1996)

[16] M. Weygang *et al.*, Biophys J **76**, 458-468 (1999)

[17] H. Mohwald *et al.*, Jpn J Appl Phys **34**, 3906-13 (1995)

[18] S. Sivasankar, PhD thesis, University of Illinois at Urbana-Champaign, USA (2001)

[19] O. Konovalov *et al.*, Eur Biophys J, in press (2002)

[20] M. Weik *et al.*, Proc Natl Acad Sci USA **97**, 623-8 (2000)

[21] Parratt32, The Reflectivity Tool, Berlin Neutron Scattering Center , Hahn-Meitner-Institut Berlin, http://www.hmi.de/bensc/software/refl/parratt/parratt.html

[22] S. Bardon *et al.*, Phys Rev E, **59**, 6808-6818 (1999)

[23] B. M. Matthews, J Mol Biol **33**, 491-497 (1968)

[24] S. Pokutta *et al.*, J Eur J Biochem **223**, 1019-1026 (1994)